

# **Cellulose-metallothionein biosorbent for removal of Pb(II) and Zn(II) from polluted water**

Wilson Mwandira<sup>a</sup>, Kazunori Nakashima<sup>b\*</sup>, Yuki Togo<sup>a</sup>, Tsutomu Sato<sup>b</sup>, Satoru Kawasaki<sup>b</sup>

<sup>a</sup>Graduate School of Engineering, Hokkaido University, Kita 13, Nishi 8, Kita-Ku, Sapporo 060-8628, Japan

<sup>b</sup>Faculty of Engineering, Hokkaido University, Kita 13, Nishi 8, Kita-Ku, Sapporo 060-8628, *Japan*

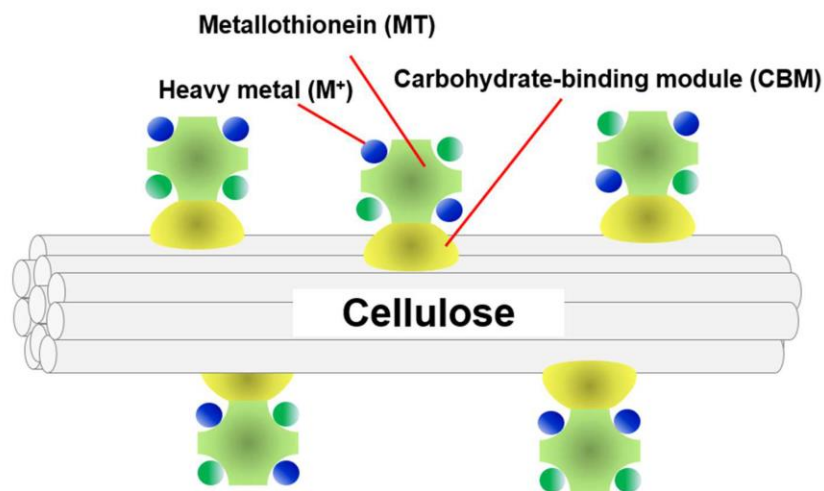
\*Corresponding Author: [nakashima@geo-er.eng.hokudai.ac.jp](mailto:nakashima@geo-er.eng.hokudai.ac.jp)

## 1 **1. Introduction**

2 Heavy metals have become a predominant contaminant of water because of constant  
3 growth in industrialization and urbanization (Chen et al., 2018). Once toxic heavy metals,  
4 such as lead (Pb) and zinc (Zn), enter the human body, they accumulate and cause various  
5 health problems. Lead has no known beneficial effects on human health, whereas Zn is  
6 essential (Zoroddu et al., 2019). However, Zn is toxic at high concentrations (Baran et al.,  
7 2018). Lead causes neurodevelopment disorders and Zn imparts an undesirable astringent  
8 taste to water, and both should be removed from drinking water (World Health Organization,  
9 2017).

10 To date, toxic trace elements have been removed by conventional water treatment  
11 methods which include coagulation, flocculation, clarification, and filtration, and followed by  
12 disinfection (Gitis and Hankins, 2018; Singh et al., 2018). However, many of these  
13 techniques are suboptimal. Biosorption has emerged as an alternative method that is efficient,  
14 simple, and specific (Singh et al., 2018). The biosorption process involves interaction of a  
15 solid phase (biosorbent) with a liquid phase (water) containing the dissolved species to be  
16 adsorbed (metal ions). Biosorbents effectively remove heavy metals from water (Fakhre and  
17 Ibrahim, 2018). Cellulose is attractive as a biosorbent because it is stable, inert, and the most  
18 abundant polymer on Earth (Abouzeid et al., 2019). However, natural cellulose has not been  
19 used as a biosorbent because of its low metal-ion adsorption capacity (Hokkanen et al.,  
20 2016). To address this challenge, we have developed a functional cellulose modified with  
21 metallothionein (MT), which adsorbs metal ions, by using a carbohydrate-binding module  
22 (CBM) as a binder.

23 In this research, we constructed a biosorbent by fusion protein of MT from  
24 *Synechococcus elongatus* and CBM from *Clostridium thermocellum* (Figure 1). MTs are a  
25 group of well-conserved proteins that act as antioxidants. They are found in all living  
26 organisms and contain a sulfhydryl group that bind to heavy metals (Chaudhary et al., 2018;  
27 Mekawy et al., 2018). However, MT would not be easy to recover after dispersion. To  
28 address this, we investigated modifying MT by fusing it with CBM. Because CBM binds to  
29 cellulose by hydrophobic interaction (Chang et al., 2018), the cellulose-MT-CBM biosorbent  
30 would be stable and easily recycled (Yunus and Tsai, 2015). Although peptide-based  
31 biosorbents have been previously suggested for water treatment (Xu et al., 2002), our  
32 biosorbent is unique in that it can be prepared in a single-step without protein purification by  
33 using cellulose-binding ability of CBM. The MT can adsorb various toxic trace elements that  
34 may be present in polluted water. We have investigated the removal of toxic metal ions,  
35 which are contained in real mine wastewater, by using a novel biosorbent.



36

37

**Figure 1.** Illustration of cellulose-MT-CBM.

## 38 2. Materials and methods

## 39 2.1. Plasmid construction and protein expression

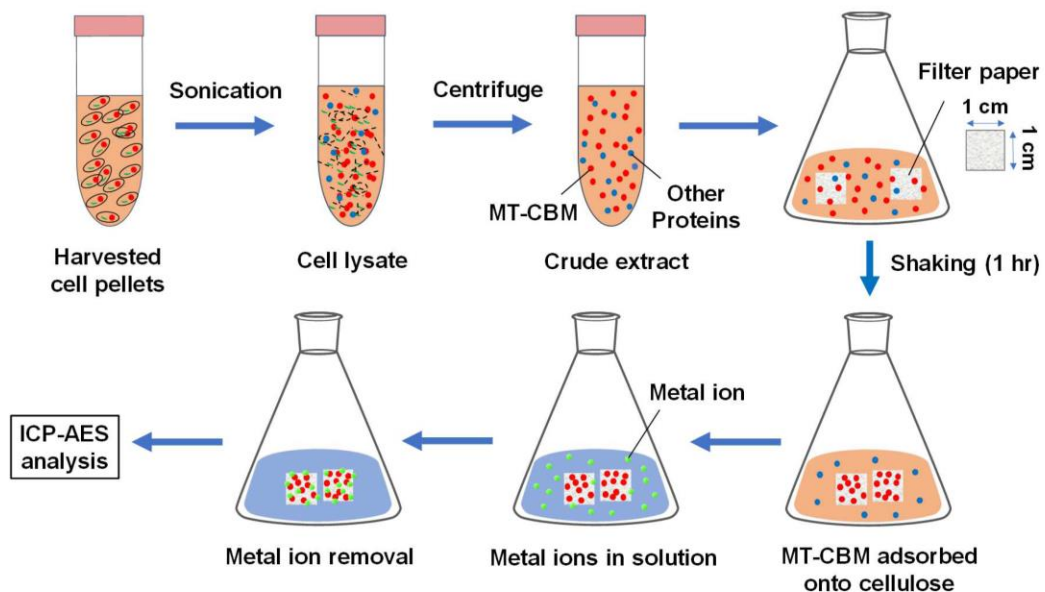
40 The gene for MT from *S. elongatus* PCC7942 (Shi et al., 1992) was synthesized by  
41 Eurofins Genomics (Tokyo, Japan). Genomic DNA from *C. thermocellum* NBRC 103400  
42 was obtained from NBRC (Kisarazu, Japan). The polymerase chain reaction (PCR) was  
43 performed using PrimeSTAR<sup>®</sup> HS DNA polymerase (Takara Bio Inc., Otsu, Japan) with the  
44 oligonucleotide primers (Eurofins Genomics) listed in Table S1. The gene for MT was  
45 amplified from the vector containing the synthesized MT gene using primers MT-F and MT-  
46 R. The gene for CBM 3 (Hong et al., 2007) was cloned from genomic DNA of *C.*  
47 *thermocellum* using the primers CBM-F and CBM-R. The genes of MT and CBM were  
48 fused by overlap PCR using the primers OL-F, OL-R, IF-F, and IF-R. The amplified gene  
49 was inserted into pET-15b vector (Merck Biosciences GmbH, Schwalbach Ts., Germany),  
50 which was cut by *Nco* I and *Xho* I, using an In-Fusion HD Cloning Kit to obtain the pET-  
51 MT-CBM vector (Figure S1). The nucleotide sequence of the MT-CBM fusion gene (648 bp)  
52 was verified by DNA sequencing (Eurofins Genomics).

53 To express the target protein, *Escherichia coli* BL21(DE3) strain (Nippon Gene Co. Ltd,  
54 Toyama, Japan) was transformed with the pET-MT-CBM vector. The transformant was  
55 grown at 37°C in Luria-Bertani (LB) medium containing 100 µg/mL ampicillin. When the  
56 optical density of the culture medium measured at a wavelength of 600 nm (OD<sub>600</sub>) reached  
57 0.45, the expression of the protein was induced by adding isopropyl β-D-1-  
58 thiogalactopyranoside (IPTG, final concentration of 1 mM) to the medium and culturing at  
59 15°C for 24 h. The bacterial cells expressing the proteins were harvested by centrifugation at  
60 8,000 ×g for 10 min and lysed by ultrasonication at 30 kHz for 5 min (Vibra-Cell<sup>™</sup> VCX  
61 130, Sonics & Materials, Inc., Newtown, USA). After centrifugation of the cell lysate at  
62 8,000 ×g for 10 min, the supernatant was recovered and used directly in biosorption studies.

63

## 64 2.2. Preparation of the cellulose-MT-CBM biosorbent

65 Biosorption of the protein onto cellulose is illustrated in Figure 2. To immobilize the  
66 MT-CBM fusion protein on cellulose and obtain the cellulose-MT-CBM biosorbent,  
67 Whatman filter paper No. 1 was cut into rectangular pieces (1 g) and then suspended in 5 mL  
68 of the crude protein mixture (protein concentration of 250  $\mu\text{g}/\text{mL}$ ) obtained in Section 2.1 for  
69 2 h at 25°C. The filter paper and cellulose-MT-CBM biosorbent were analyzed by using  
70 attenuated total reflectance Fourier transform infrared (ATR-FTIR) (JASCO 360 FTIR  
71 Spectrometer, JASCO, Japan). The point of zero charge (pzc) for the cellulose-MT-CBM was  
72 determined by the pH drift method (Bakatula et al., 2018).



73

74 **Figure 2.** The process of immobilization of the MT-CBM protein on cellulose.

### 75 2.3. Metal ion adsorption experiments

76 A metal ion stock solution was prepared using PbCl<sub>2</sub> and ZnCl<sub>2</sub> (Wako Pure Chemical  
77 Industries Ltd, Tokyo, Japan), which were dissolved in distilled water. Solutions with  
78 different final concentrations of the metal ions were obtained by dilution of the stock  
79 solution. Metal adsorption was investigated in batch experiments. The effect of pH (2.0–9.0)  
80 on the removal of Pb(II) and Zn(II) was investigated by mixing 1 g of the prepared biosorbent  
81 with 100 mL of a 20 mg/L metal solution in a 250 mL Erlenmeyer flask. Then, the flasks  
82 were placed on a shaker at 100 rpm for 1 h. The adsorbent was recovered by centrifugation at  
83 8,000 ×g for 10 min and the supernatant was filtered through a 0.45-μm filter. The metal ion  
84 concentration in the supernatant was measured by inductively coupled plasma atomic  
85 emission spectroscopy (ICP-AES) (ICPE-9820, Shimadzu Corporation, Kyoto, Japan). The  
86 effect of the contact time (0–60 min) was studied by varying this while keeping all other  
87 parameters fixed.

88 Biosorption was analyzed using the Langmuir isotherm model:

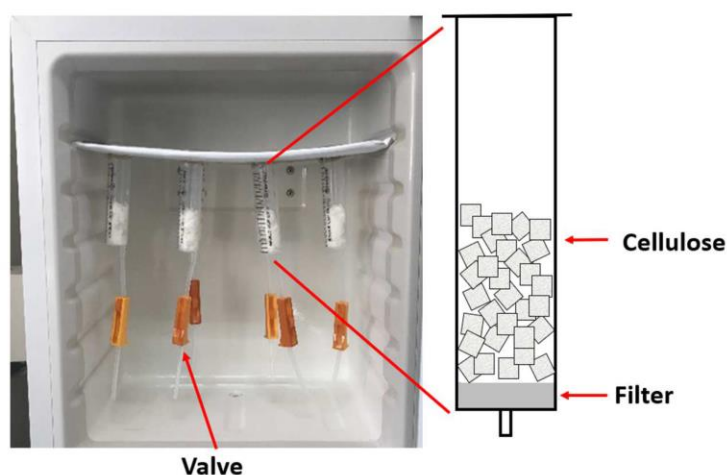
$$90 \quad Q_{\text{eq}} = \frac{Q_{\text{max}} \cdot K \cdot C_{\text{eq}}}{1 + K \cdot C_{\text{eq}}}, \quad (1)$$

91 where  $Q_{\text{eq}}$  is the quantity adsorbed (mg/g),  $C_{\text{eq}}$  is the equilibrium concentration of the  
92 adsorbate (mg/L),  $Q_{\text{max}}$  is the Langmuir constant (mg/g), and  $K$  is the equilibrium constant.

### 92 2.4. Semi-continuous adsorption system and recyclability of the cellulose-MT-CBM 93 biosorbent

94 The reusability of the adsorbent in a semi-continuous system was tested seven times with  
95 the experimental setup illustrated in Figure 3. To determine the recoverability and reusability

96 of the biosorbent, a column (syringe of mean diameter,  $D_{50} = 2.5$  cm and height,  $h = 7$  cm)  
97 was prepared by placing 2 g of cellulose in a 30-mL syringe. Then, 10 mL of crude extract  
98 containing overexpressed MT-CBM protein (total protein concentration: 250  $\mu\text{g/mL}$ ) was  
99 added to be adsorbed onto the cellulose, and the column was kept at 25°C in an incubator for  
100 1 h. After washing three times with deionized water, a Pb(II) or Zn(II) aqueous solution was  
101 allowed to percolate through the column. The filtrate was collected for metal analysis. A  
102 valve was used to regulate the flow rate of the filtrate from the column. To desorb the  
103 adsorbed metal ions, 10 mL of 20 mM EDTA buffer (pH 8) was added to the column. To  
104 regenerate the column, 10 mL of fresh MT-CBM protein was added. A column containing  
105 only cellulose was used for control experiments. Treatment of actual mine wastewater  
106 collected from Chingola, Copperbelt, Zambia was investigated using the column.



108 **Figure 3.** Setup for the cellulose-MT-CBM biosorbent regeneration experiments.

### 109 2.5. X-ray photoelectron spectroscopy analysis

110 X-ray photoelectron spectroscopy (XPS) measurements were performed by using a JPS-  
111 9200 spectrometer (JEOL Ltd, Tokyo, Japan) to explore the electronic states of Pb and Zn on

112 the biosorbent using monochromatic Mg K $\alpha$  radiation. To compensate for surface charge  
113 effects, the binding energies were calibrated using C 1s at 284.80 eV.

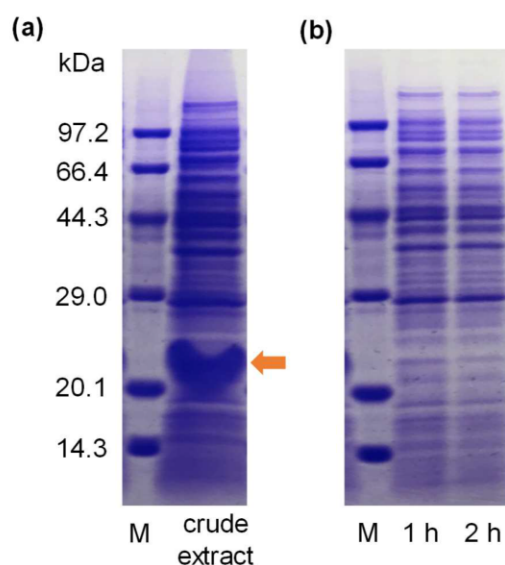
### 114 **3. Results and Discussion**

#### 115 **3.1. Verification of plasmid construction, protein expression, and protein binding ability** 116 **to cellulose**

117 Figure 4 shows the results of SDS-PAGE analysis for the protein expressed in *E. coli*  
118 BL21(DE3) and biosorption of the protein to cellulose. Figure 4(a) shows the supernatant of  
119 the cell lysate of *E. coli* expressing MT-CBM. We found that the MT-CBM was successfully  
120 expressed in a soluble form with a molecular weight of 23.1 kDa. To verify the binding  
121 ability of the MT-CBM on cellulose, filter papers were added to the cell lysate. After 1 h, the  
122 band for MT-CBM disappeared, indicating that the MT-CBM in the cell lysate was adsorbed  
123 on cellulose (Figure 4(b)). This result showed that MT-CBM could be purified using  
124 cellulose in a single step. This result is consistent with previous studies where CBM was  
125 observed to bind to cellulosic material (Hong et al., 2007). We then used the cellulose-based  
126 biosorbent (cellulose-MT-CBM) for further studies. The FTIR spectra are obtained for pure  
127 cellulose and cellulose-MT-CBM (Figure S2). The results showed that the pure cellulose had  
128 no distinguishable functional groups compared with the cellulose-MT-CBM, where broad  
129 and strong bands at 3251 cm<sup>-1</sup> (amine (-NH)), 1625 cm<sup>-1</sup> (amide group (C=O)), and 1302  
130 cm<sup>-1</sup> (C-O stretching) confirmed the presence of bound protein on the cellulose.

131





132

133 **Figure 4.** SDS-PAGE of (a) crude extract after expression of MT-CBM and (b) after addition  
 134 of filter paper to crude extract (1 h and 2 h). M: protein marker.

### 135 3.2. Metal ion adsorption experiments

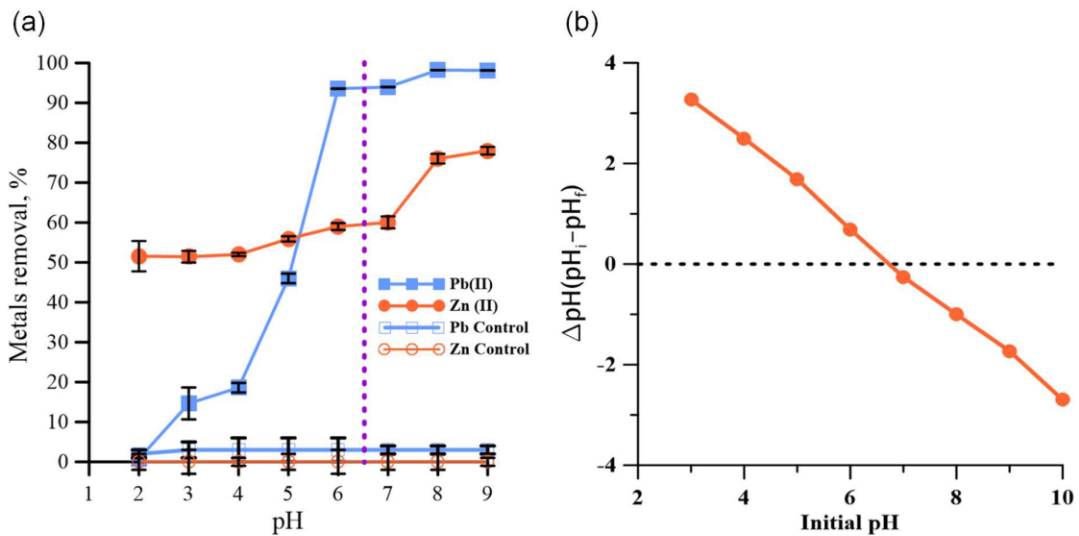
#### 136 3.2.1. The effect of contact time

137 Contact time is an important factor affecting the efficiency of biosorption because it  
 138 provides valuable information on how fast the removal process occurs. Time course of metal  
 139 ion adsorption is shown in Figure S3. Equilibrium of the biosorption of Pb(II) and Zn(II) on  
 140 the cellulose-MT-CBM reached equilibrium within 10 min. This rapid metal sorption is  
 141 highly desirable for biosorbents for practical applications.

#### 142 3.2.2. Effect of pH on metal ion adsorption

143 The effect of the initial pH of the solution on metal ion adsorption on cellulose-MT-  
 144 CBM and untreated cellulose (control) is shown in Figure 5(a). The influence of pH on the

145 biosorption of Pb(II) and Zn(II) indicated that the biosorption increased with pH. From pH  
 146 2.0 to 7.0, the percentage of Pb(II) removed increased from 0.8 % to 94 %, and that of Zn(II)  
 147 increased from 52 % to 60 %. The slightly lower biosorption yield observed for Zn(II) could  
 148 be attributed to the possible inert nature of one of the MT binding sites to Zn as reported  
 149 previously (Harrison et al., 2002).



150  
151

152 **Figure 5.** (a) Effect of pH on the adsorption of Pb(II) and Zn(II) on cellulose-MT-CBM  
 153 (biomass dosage: 10 g/L, initial metal ion concentration: 20 mg/L, temperature: room  
 154 temperature; the purple dotted line indicates the pzc of the biosorbent) and (b) pzc of the  
 155 cellulose-MT-CBM biosorbent.

156 At lower pH values, the binding sites are protonated and the metal ions are in solution  
 157 because they cannot access the binding sites on the cellulose-MT-CBM. At higher pH values,  
 158 the binding sites are deprotonated, negatively charged, and more favorable for adsorption.  
 159 The control had negligible biosorption capacity at all pH values because of a lack of binding  
 160 ability. The percentages of Pb(II) and Zn(II) removed increased significantly at pH 6.5. This

161 higher adsorption could be related to the pzc of the cellulose-MT-CBM (Fig. 5b). At pH >  
162 pzc, the biosorption of Pb(II) and Zn(II) to the biosorbent is favorable because of the  
163 presence of negatively charged functional groups of the protein (Bakatula et al., 2018).  
164 Therefore, negatively charged functional groups at pH 6.5 would be able to attract and  
165 sequester positively charged metal ions.

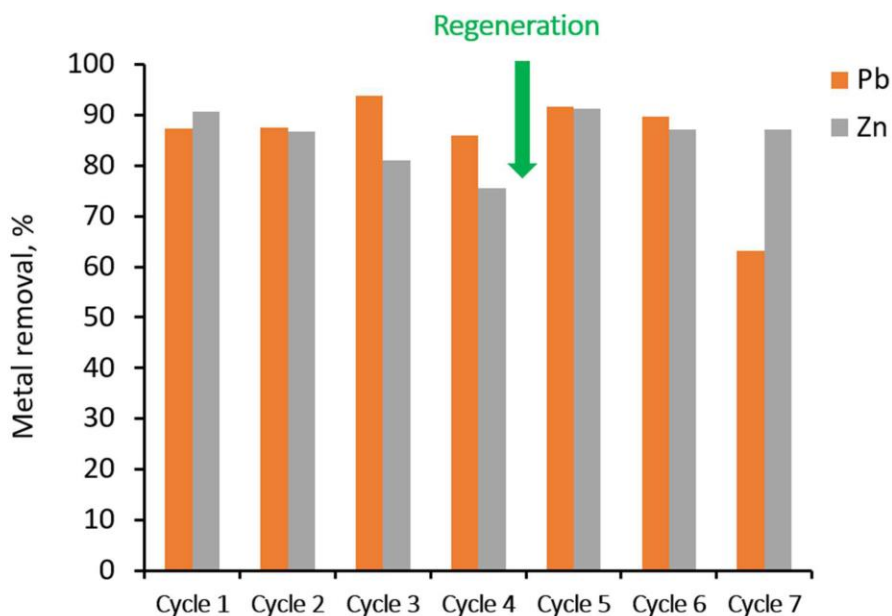
### 166 **3.2.3. Biosorption capacity**

167 The adsorption isotherm was studied to understand the equilibrium distribution of Pb(II)  
168 and Zn(II) between the aqueous phase and surface of the biosorbent. The Langmuir isotherm  
169 model was suitable for the experimental data as shown by a good fit with model data (Figure  
170 S4). This indicates that the biosorption of Pb(II) and Zn(II) onto the cellulose-MT-CBM takes  
171 place via a monolayer mechanism. The maximum biosorption capacities for Pb(II) and Zn(II)  
172 were higher than those obtained with other cellulose-based biosorbents. For Pb (II), Dhir and  
173 Kumar, (2010) found a  $Q_{\max}$  value of 41.84 mg/g for wheat straw compared with 39.02 mg/g  
174 for the cellulose-MT-CBM in the present study. For Zn (II), Tian et al., (2017) found a  $Q_{\max}$   
175 value of 5.38 mg/g on a cellulose nanofibril aerogel compared with 29.28 mg/g on the  
176 cellulose-MT-CBM in the present study. These results indicate that the cellulose-MT-CBM  
177 biosorbent can be used for the removal of heavy metals from water.

### 178 **3.3. Recyclability of the cellulose-MT-CBM biosorbent**

179 Recyclability of the cellulose-MT-CBM biosorbent was examined because waste has a huge  
180 negative impact on the natural environment. The results for the biosorbent recyclability  
181 experiments are shown in Figure 6. The cellulose-MT-CBM was regenerated seven times and  
182 the bound metal ion was desorbed by 20 mM EDTA. In cycle 4, the adsorption ability  
183 slightly decreased. The adsorption ability could be restored by addition of MT-CBM to the

184 cellulose, which resulted in an increase in the metal biosorption. These results show that the  
185 biosorbent could be used for multiple metal sorption/desorption cycles without any  
186 significant loss in its efficiency.



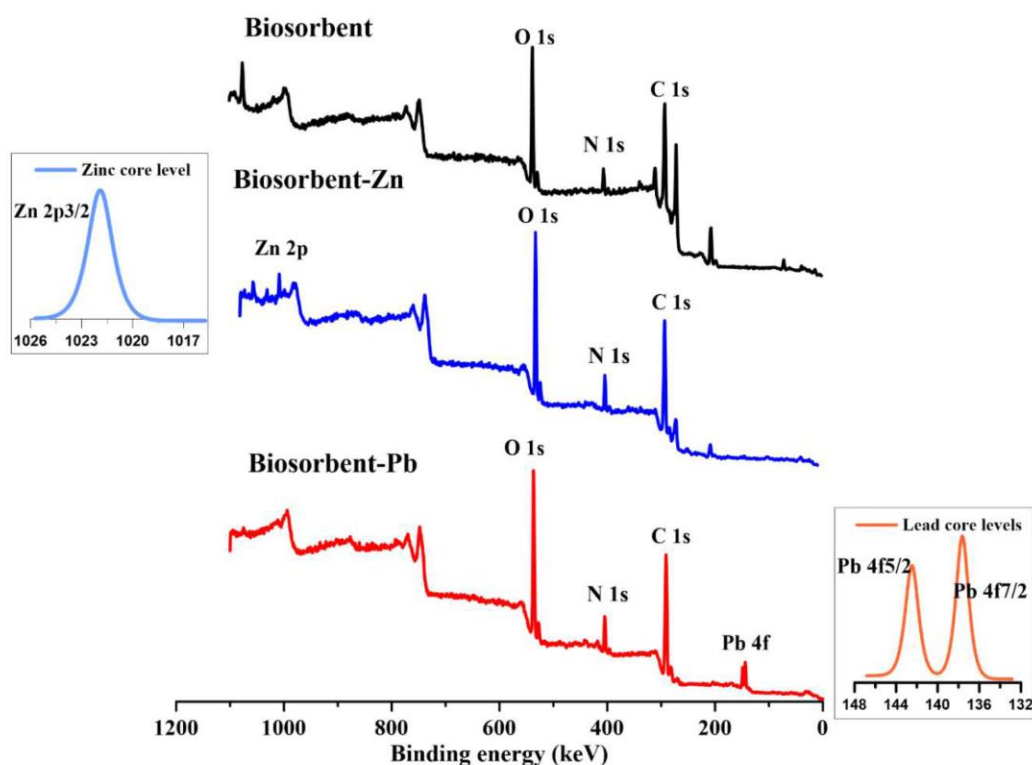
187

188 **Figure 6.** Pb(II) and Zn(II) removal efficiencies of the cellulose-MT-CBM biosorbent for  
189 different cycles (initial metal ion concentration: 20 mg/L, pH: 6.5, temperature: room  
190 temperature).

### 191 3.4. XPS analysis

192 XPS measurements of cellulose-MT-CBM after metal adsorption were performed to  
193 confirm the electronic state(s) of Pb(II) and Zn(II) on the biosorbent. XPS wide scan spectra  
194 of cellulose-MT-CBM before and after Pb(II) and Zn(II) adsorption depicted core levels of C  
195 1s, O 1s, N 1s, Pb 4d, and Zn 2p (Figure 7). Two new peaks at 141 and 136 eV appeared after  
196 Pb (II) adsorption, which were attributed to the Pb 4f orbital (Qiao et al., 2019). One new  
197 peak at 1022 eV was attributed to the Zn 2p orbital (Zhou et al., 2016). These results indicate

198 that Pb(II) and Zn(II) are adsorbed on the biosorbent. The source of N 1s is the MT-CBM  
199 protein bound on the cellulose.



200

201 **Figure 7.** Typical XPS wide scan spectra of the cellulose-MT-CBM before and after Pb(II)  
202 and Zn(II) adsorption.

203 Metal adsorption by cellulose-MT-CBM could be attributed to the formation of N:  
204 Pb<sup>2+</sup> and N: Zn<sup>2+</sup> complexes, in which a lone pair of electrons from the N atom in -NH<sub>2</sub> group  
205 is donated to a shared bond between the nitrogen atom and Pb<sup>2+</sup> or Zn<sup>2+</sup>. Additionally, the  
206 oxygen atom could be responsible for heavy metal removal via ionic interactions with Pb<sup>2+</sup>  
207 and Zn<sup>2+</sup>. The O 1s peak at 532.29 eV was modeled after curve fitting and attributed to the  
208 oxygen-rich functional groups such as -COOH group, which interact with heavy metals to  
209 form O: Pb<sup>2+</sup> or O: Zn<sup>2+</sup>. The XPS results confirm the FTIR data that identified organic  
210 functional groups such as -NH<sub>2</sub> and -COOH groups on the biosorbent (Figure S2).

211 Furthermore, the removal of heavy metals by the cellulose-MT-CBM occurs via heavy metal  
 212 complexation with the thiol group of cysteine-rich MTs (Diep et al., 2018) and ion exchange  
 213 with the O atom in the biosorbent as previously reported (Jana et al., 2016).

### 214 **3.5. Treatment of actual mine wastewater by the cellulose-MT-CBM biosorbent**

215 To demonstrate industrial application of the cellulose-MT-CBM, the biosorbent was used  
 216 to treat contaminated surface water from an industrial source. The Mushishima stream in  
 217 Chingola, Zambia, which flows into the Kafue River, is affected by effluent from the active  
 218 Nchanga Mine (Sracek et al., 2012). It is essential to evaluate the performance of the  
 219 biosorbent in a multi-metal system that reflects real effluent as opposed to simulated metal  
 220 ion solutions. Table 1 shows the water quality data obtained before and after treatment with  
 221 the cellulose-MT-CBM using the setup illustrated in Figure 3. Treated water from the site  
 222 showed complete removal of toxic elements with below the detection limit of ICP-AES.  
 223 These results show that the cellulose-MT-CBM is effective and be applied in the mining  
 224 industry as a clean-up technique.

225

226 **Table 1.** Concentrations of metal ions in mine wastewater before and after treatment with  
 227 the cellulose-MT-CBM biosorbent.

Toxic trace elements of concern	Before (mg/L)	After (mg/L)	WHO acceptable Limit (mg/L)
Pb	0.19	< 0.001	0.01
Cu	14.56	< 0.001	2.00
Ni	7.74	< 0.001	0.07
Cd	0.34	< 0.001	0.10

228

#### 229 **4. Conclusion**

230 In this study we developed a novel biosorbent composed of cellulose and a fusion protein.  
231 The fusion protein was constructed from metallothionein (MT) and a carbohydrate-binding  
232 module (CBM), where CBM binds to cellulose and MT captures heavy metal ions in solution.  
233 The biosorbent had maximum biosorption capacities of 39.02 mg/g for Pb(II) and 29.28 mg/g  
234 for Zn(II) ions. The resulted cellulose-MT-CBM biosorbent showed regeneration and  
235 reusability after repeated using seven times in a semi-continuous system. The biosorbent was  
236 applied to purify multiparameter contaminated real mining wastewater and showed complete  
237 removal of Pb(II), Cu(II), Ni(II), and Cd(II) to below detection limit. Because of these  
238 capabilities, this biosorbent has great potential for efficient removal of toxic trace elements  
239 from polluted water.

240

241 **Declarations of interest: none**

242 **Appendix A. Supplementary material**

243

244 **Acknowledgments**

245 This work was partly supported by Japan Society for the Promotion of Science (JSPS)  
246 KAKENHI (grant number JP18H03395) and Japan Science and Technology Agency (JST),  
247 Japan International Cooperation Agency (JICA), and Science and Technology Research  
248 Partnership for Sustainable Development (SATREPS). We thank the Laboratory of XPS  
249 analysis, Joint-use facilities, Hokkaido University, supported by the Material Analysis and  
250 Structure Analysis Open Unit (MASAOU) for XPS analysis.



251 **REFERENCES**

- 252 Abouzeid, R.E., Khiari, R., El-Wakil, N., Dufresne, A., 2019. Current State and New Trends  
253 in the Use of Cellulose Nanomaterials for Wastewater Treatment. *Biomacromolecules*  
254 20, 573–597. <https://doi.org/10.1021/acs.biomac.8b00839>
- 255 Bakatula, E.N., Richard, D., Neculita, C.M., Zagury, G.J., 2018. Determination of point of  
256 zero charge of natural organic materials. *Environ. Sci. Pollut. Res.* 25, 7823–7833.  
257 <https://doi.org/10.1007/s11356-017-1115-7>
- 258 Baran, A., Wieczorek, J., Mazurek, R., Urban, K., Klimkiewicz-pawlas, A., 2018. Potential  
259 ecological risk assessment and predicting zinc accumulation in soils 435–450.  
260 <https://doi.org/10.1007/s10653-017-9924-7>
- 261 Chang, F., Xue, S., Xie, X., Fang, W., Fang, Z., Xiao, Y., 2018. Carbohydrate-binding  
262 module assisted purification and immobilization of  $\beta$ -glucosidase onto cellulose and  
263 application in hydrolysis of soybean isoflavone glycosides. *J. Biosci. Bioeng.* 125, 185–  
264 191. <https://doi.org/10.1016/J.JBIOOSC.2017.09.001>
- 265 Chaudhary, K., Agarwal, S., Khan, S., 2018. Role of Phytochelatins (PCs), Metallothioneins  
266 (MTs), and Heavy Metal ATPase (HMA) Genes in Heavy Metal Tolerance, in:  
267 *Mycoremediation and Environmental Sustainability*. Springer, Cham, pp. 39–60.  
268 [https://doi.org/10.1007/978-3-319-77386-5\\_2](https://doi.org/10.1007/978-3-319-77386-5_2)
- 269 Chen, L., Zhou, S., Shi, Y., Wang, C., Li, B., Li, Y., Wu, S., 2018. Heavy metals in food  
270 crops , soil , and water in the Lihe River Watershed of the Taihu Region and their  
271 potential health risks when ingested. *Sci. Total Environ.* 615, 141–149.  
272 <https://doi.org/10.1016/j.scitotenv.2017.09.230>
- 273 Dhir, B., Kumar, R., 2010. Adsorption of Heavy Metals by *Salvinia* Biomass and  
274 Agricultural Residues. *Int. J. Environ. Res* 4, 427–432.
- 275 Diep, P., Mahadevan, R., Yakunin, A.F., 2018. Heavy metal removal by bioaccumulation

276 using genetically engineered microorganisms. *Front. Bioeng. Biotechnol.* 6: 157.  
277 <https://doi.org/10.3389/fbioe.2018.00157>

278 Fakhre, N.A., Ibrahim, B.M., 2018. The use of new chemically modified cellulose for heavy  
279 metal ion adsorption. *J. Hazard. Mater.* 343, 324–331.  
280 <https://doi.org/10.1016/j.jhazmat.2017.08.043>

281 Gitis, V., Hankins, N., 2018. Water treatment chemicals : Trends and challenges 25, 34–38.  
282 <https://doi.org/10.1016/j.jwpe.2018.06.003>

283 Harrison, M.D., Sadler, P.J., Robinson, A.K., Robinson, N.J., Parkinson, J.A., Cavet, J.S.,  
284 Blindauer, C.A., 2002. A metallothionein containing a zinc finger within a four-metal  
285 cluster protects a bacterium from zinc toxicity. *Proc. Natl. Acad. Sci.* 98, 9593–9598.  
286 <https://doi.org/10.1073/pnas.171120098>

287 Hokkanen, S., Bhatnagar, A., Sillanpää, M., 2016. A review on modification methods to  
288 cellulose-based adsorbents to improve adsorption capacity. *Water Res.* 91, 156–173.  
289 <https://doi.org/10.1016/j.watres.2016.01.008>

290 Hong, J., Ye, X., Zhang, Y.H.P., 2007. Quantitative determination of cellulose accessibility  
291 to cellulase based on adsorption of a nonhydrolytic fusion protein containing CBM and  
292 GFP with its applications. *Langmuir* 23, 12535–12540.  
293 <https://doi.org/10.1021/la7025686>

294 Jana, A., Bhattacharya, P., Sarkar, S., Majumdar, S., Ghosh, S., 2016. An ecofriendly  
295 approach towards remediation of high lead containing toxic industrial effluent by a  
296 combined biosorption and microfiltration process: a total reuse prospect. *Desalin. Water*  
297 *Treat.* 57, 5498–5513. <https://doi.org/10.1080/19443994.2015.1004596>

298 Mekawy, A.M.M., Assaha, D.V.M., Munehiro, R., Kohnishi, E., Nagaoka, T., Ueda, A.,  
299 Saneoka, H., 2018. Characterization of type 3 metallothionein-like gene (OsMT-3a)  
300 from rice, revealed its ability to confer tolerance to salinity and heavy metal stresses.

301 Environ. Exp. Bot. 147, 157–166. <https://doi.org/10.1016/j.envexpbot.2017.12.002>

302 Qiao, W., Zhang, Y., Xia, H., Luo, Y., Liu, S., Wang, S., Wang, W., 2019.

303 Bioimmobilization of lead by *Bacillus subtilis* X3 biomass isolated from lead mine soil

304 under promotion of multiple adsorption mechanisms. R. Soc. Open Sci. 6.

305 <https://doi.org/10.1098/rsos.181701>

306 Shi, J., Lindsay, W.P., Huckle, J.W., Morby, A.P., Robinson, N.J., 1992. Cyanobacterial

307 metallothionein gene expressed in *Escherichia coli* Metal-binding properties of the

308 expressed protein. FEBS Lett. 303, 159–163. [https://doi.org/10.1016/0014-](https://doi.org/10.1016/0014-5793(92)80509-F)

309 [5793\(92\)80509-F](https://doi.org/10.1016/0014-5793(92)80509-F)

310 Singh, N.B., Nagpal, G., Agrawal, S., Rachna, 2018. Water purification by using Adsorbents:

311 A Review. Environ. Technol. Innov. 11, 187–240.

312 <https://doi.org/10.1016/j.eti.2018.05.006>

313 Sracek, O., Křibek, B., Mihaljevič, M., Majer, V., Veselovský, F., Vencelides, Z., Nyambe,

314 I., 2012. Mining-related contamination of surface water and sediments of the Kafue

315 River drainage system in the Copperbelt district, Zambia: An example of a high

316 neutralization capacity system. J. Geochemical Explor. 112, 174–188.

317 <https://doi.org/10.1016/j.gexplo.2011.08.007>

318 Tian, C., Qing, Y., Luo, S., Wu, Q., She, J., Wu, Y., 2017. Reusable and cross-linked

319 cellulose nanofibrils aerogel for the removal of heavy metal ions. Polym. Compos. 39,

320 4442–4451. <https://doi.org/10.1002/pc.24536>

321 World Health Organization, 2017. Guidelines for drinking-water quality.

322 [https://doi.org/10.1016/S1462-0758\(00\)00006-6](https://doi.org/10.1016/S1462-0758(00)00006-6)

323 Xu, Z., Bae, W., Mulchandani, A., Mehra, R.K., Chen, W., 2002. Heavy metal removal by

324 novel CBD-EC20 sorbents immobilized on cellulose. Biomacromolecules 3, 462–465.

325 <https://doi.org/10.1021/bm015631f>

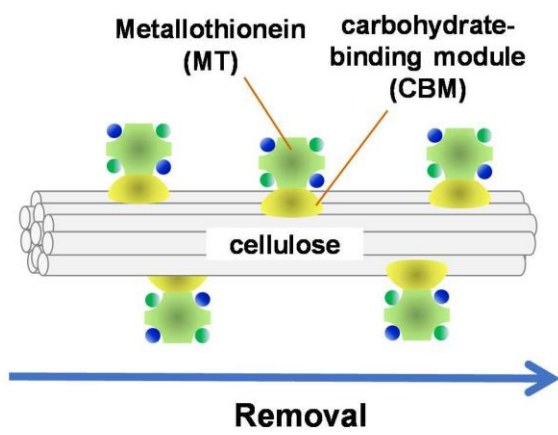
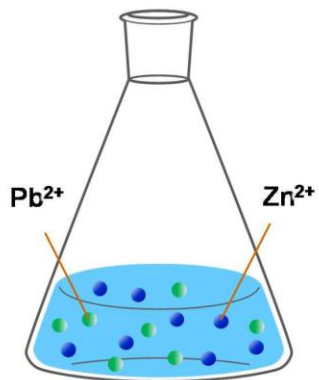
326 Yunus, I.S., Tsai, S.-L., 2015. Designed biomolecule–cellulose complexes for palladium  
327 recovery and detoxification. *RSC Adv.* 5, 20276–20282.  
328 <https://doi.org/10.1039/C4RA16200E>

329 Zhou, Y., Zhang, Z., Zhang, J., Xia, S., 2016. New insight into adsorption characteristics and  
330 mechanisms of the biosorbent from waste activated sludge for heavy metals. *J. Environ.*  
331 *Sci. (China)* 45, 248–256. <https://doi.org/10.1016/j.jes.2016.03.007>

332 Zoroddu, M.A., Aaseth, J., Crisponi, G., Peana, M., Nurchi, V.M., 2019. The essential metals  
333 for humans: A brief overview Maria. *J. Inorg. Biochem.* #pagerange#.  
334 <https://doi.org/10.1016/j.jinorgbio.2019.03.013>

335

**Contaminated water**



**Treated water**

